Received: 15 January 2020 | Revised: 23 August 2020 | Accepted: 28 September 2020

IET Energy Systems Integration

DOI: 10.1049/esi2.12008

ORIGINAL RESEARCH PAPER

Hybrid power plant bidding strategy for voltage stability improvement, electricity market profit maximization, and congestion management

Sahand Ghavidel[1] | Amin Rajabi[1] | Mojtaba Jabbari Ghadi[1] | Ali Azizivahed[1] | Li Li[1] | Jiangfeng Zhang[2]

[1]School of Electrical and Data Engineering, University of Technology Sydney, Broadway, NSW, Australia

[2]Department of Automotive Engineering, Clemson University, Greenville, SC, USA

Correspondence

Sahand Ghavidel, School of Electrical and Data Engineering, University of Technology Sydney, Broadway, NSW 2007, Australia.
Email: sahand.ghavideljirsaraie@student.uts.edu.au

Abstract

This article models a hybrid power plant (HPP), including a compressed air energy storage (CAES) aggregator with a wind power aggregator (WPA) considering network constraints. Three objective functions are considered including electricity market profit maximization, congestion management, and voltage stability improvement. In order to accurately model the WPA, pitch control curtailment wind power levels are also added to the wind power generator models. To optimize all the mentioned objective functions, a multi-objective Pareto front solution strategy is used. Finally, a fuzzy method is used to find the best compromise solution. The proposed approach is tested on a realistic case study based on an electricity market and wind farm located in Spain, and IEEE 57-bus test system is used to evaluate the network constraint effects on the HPP scheduling for different objective functions.

1 | INTRODUCTION

Owing to the non-dispatchable, unstable, and stochastic nature of wind power, it is a challenging issue for wind power aggregators (WPAs) and producers to participate in electric power markets, especially competing with traditional fuel-based power plants. Therefore, adopting an optimal strategy for WPAs to overcome such difficulties is of importance.

Currently, energy storage systems, especially CAES, have attracted the significant attention of the researchers as a potential and mature, extensive scale energy storage technology with the ability of operation as a gas turbine when the pressured air is depleted in the reservoir [1]. Merchant CAES units can provide the role of an energy shifter when there are many variations in the hourly price of energy in the market. However, their capability of working as a gas turbine, in the simple cycle mode, makes large-scale CAES technology utterly different than other types of storage systems. A more optimized scheduling approach can be reached for CAES by catching sparks of energy prices in the market while following their predefined schedule [2].

The network constraints can also affect the scheduling of the generators and storage units like WPA and CAES. Depending on the objective function that the decision-maker aims to optimize, the power scheduling of the mentioned aggregators can be different. For example, if the objective function is to optimize the electricity market profit, the aggregators would follow the price of electricity markets, but if the objective function is to minimize the congestion, the scheduling would be different to change the power flow through the network.

1.1 | Literature review

In this regard, some researchers study the best strategies of CAES self-scheduling to formulate their income from energy arbitrage in different electric power markets [3]. As an illustration, a co-optimized model for the CAES dispatching is presented in [4] to highlight the importance of energy and reserves arbitrage provision in various U.S. electric power markets. Authors in [2] propose a risk-constrained bidding

approach for the day-ahead (DA) market participation of a commercial CAES plant.

Besides, a number of studies present offering strategies for WPA participation in the electric power markets. Reference [5] proposes a WPA offering strategy for different electricity markets to consider the uncertainties of wind power and the price in different electricity markets. Reference [6] proposes an offering strategy for a price-maker WPA to participate in a DA electricity market. A similar study has been accomplished in [7] for a WPA as a price-maker in the balancing market while being a price-taker in the DA market. A hybrid stochastic-information gap decision theory algorithm is used to handle the wind uncertainty and power equipment failure in [8, 9].

Besides, some articles propose offering strategies for joint operation of WPAs with other producers. In this regard, authors in [10] formulate offering an approach to a thermal unit aggregator to participate in the market in collaboration with the WPA. A similar study is accomplished in [11] for a hybrid WPA and pumped-storage system considering uncertainties of wind generation and electricity prices in the market. Reference [4] investigates wind uncertainty effects on the stored energy of pumped-hydro in the future U.K. system. A CVaR model-based offering strategy is proposed in [12] for a joint wind-hydro aggregator to handle the financial risk of participating in the DA market. Two different models for aggregation of a WPA with a CAES and a gas turbine unit are presented in [13]. A flexible load to support imbalances of WPA is employed in [14] to battle uncertainties of participation in DA electric power market. The model proposed in [15] aims at minimizing the total operating costs (i.e. including imbalance fines) as a result of wind power over/underestimation. The strategy is formulated based on critical peak pricing to model the demand response programme involved in the DA participation approach. In [16], all the electricity markets (i.e. including DA, intraday and balancing markets) are considered in the joint offering strategy of a WPA and a demand response resource.

Some research has been accomplished in the case of network constrained offering strategies of different aggregators. Such the approach considering uncertainties of wind power and loads is studied in [17, 18] to present a corrective voltage control that can cope with voltage instability resulted from severe contingencies. A similar approach using a probabilistic optimal power flow is presented in [19] to set a compromise among involvement of wind, photovoltaic, and plug-in electric vehicle energy sources in the form of a hybrid power plant (HPP), while the probability distribution factor required to generate the stochastic powers is based on Monte Carlo simulation. A security-constrained optimal power flow problem incorporating thermal power units and wind generators, considering Weibull probability function to model wind power uncertainties, is solved in [20].

1.2 | Approach and contribution

The participation of an HPP (including a WPA and a CAES aggregator) in the DA electricity market considering network constraints is proposed. The CAES unit is capable of working as a gas turbine in the simple cycle mode. The proposed methodology uses CAES to control uncertainties of the price in different electricity markets as well as wind power forecasting, while WPA assists the CAES aggregator to schedule simple cycle mode, charging and discharging more economically. A multi-objective mixed integer nonlinear programming problem for three objective functions including electricity market profit maximization, voltage stability improvement, and congestion management is formulated which is solved using an improved Jaya algorithm [21]. The contributions of the paper are given as follows:

- An HPP including a CAES aggregator and a WPA is modelled considering network constraints.
- Three objective functions are considered, including electricity market profit maximization, congestion management, and voltage stability improvement.
- In order to properly model the WPA, pitch control for wind power curtailment is added to wind generator modelling.
- The IEEE 57-bus system is used to integrate WPA and CAES, to validate the proposed bidding strategy, and to analyse the effects of network constraint on the HPP scheduling for different objective functions, while the real data of wind farm and electricity market located in Spain are used.

1.3 | Paper organization

The rest of the articler is structured as follows: Section 2 provides the problem formulation of three objective functions including profit maximization, voltage stability, and congestion management. Section 3 deliberates the case study and delivers the results. To conclude, Section 4 summarizes the achievement of the article.

2 | PROBLEM FORMULATION

Three objective functions are considered including profit maximization, voltage stability, and congestion management. The first objective function is profit maximization, which is equal to the HPP revenue minus its total operating costs.

$$\max_{\Theta h_{t,s}} \mathcal{Z}_1$$
$$\mathcal{Z}_1 = \sum_{s=1}^{N_s} \sum_{t=1}^{N_T} \pi_s \left[\rho_{t,s}^{DA} . Ph_{t,s}^{DA} - OC_{t,s} \right] \quad (1)$$

where $\Theta h_{t,s} = \{Ph_{t,s}^{DA}, Uw_{t,s}^{DA}, Pw_{t,s}^{DA}, Pc_{t,s}^{DA}, Pc_{t,s}^{DA,Dis}, Pc_{t,s}^{DA,Sim}, Pc_{t,s}^{DA,Cha}, Uc_{t,s}^{DA,Di}, \beth_t, Uc_{t,s}^{DA,Sim}, Uc_{t,s}^{DA,Cha}, Ec_{t,s}^{DA}\}$, are the variables related to the HPP optimization problem. The CAES operational cost $OC_{t,s}$ is calculated in Equation (16) as the function of power dispatch in charging, discharging, and simple cycle modes.

The first objective function (Equation 1) is subject to the combined and individual constraints in the case of merchant CAES unit and WPA.

The limit of HPP offer in the DA market is defined as follows:

$$Ph_{t,s}^{DA} = Pw_{t,s}^{DA} + Pc_{t,s}^{DA} \quad \forall t,\ \forall s \tag{2}$$

where $Pw_{t,s}^{DA}$ and $Pc_{t,s}^{DA}$ are limited to the following constraints:

$$0 \le Pw_{t,s}^{DA} \le Pw^{Max} \quad \forall t,\ \forall s \tag{3}$$

$$-Pc_{Com}^{Max} \le Pc_{t,s}^{DA} \le Pc_{Exp}^{Max} \quad \forall t,\ \forall s \tag{4}$$

Noteworthy, getting positive/negative values of $Pc_{t,s}^{DA}$ in Equation (4) permits HPP to both buy/sell in the DA market.

In order to properly model the WPA, the pitch angle control is added to wind generators using Equation (5) to curtail the wind power level. Equation (5) refers to how the wind power PDF is modified after curtailment [22]. The pitch power control is a mechanism using changes in the blade pitch angle in the wind turbines to reduce the power generation. It is implemented to cut the extra power generation when the generated wind power is more than the forecasted value.

The wind curtailment level is carried out based on the 'discretized probability density function'.

$$\bar{\pi} w_{t,h}^{DA} = \begin{cases} \pi w_{t,h}^{DA} & if \quad g_{t,h}^{DA} < g_{t,\beth_t}^{DA} \\ \sum_{j \ge \beth_t} \pi w_{t,j}^{DA} & if \quad g_{t,h}^{DA} = g_{t,\beth_t}^{DA} \\ 0 & if \quad g_{t,h}^{DA} > g_{t,\beth_t}^{DA} \end{cases} \tag{5}$$

where $g_{t,\beth_t}^{DA}$ is the maximum hourly caps further than which all the wind power will be dropped, and $\beth_t$ values are between one and seven in this paper. $\bar{\pi} w_{t,h}^{DA}$ is the probability of wind power equal to $g_{t,h}^{DA}$ when the wind is curtailed. $\pi w_{t,h}^{DA}$ is the probability of wind power equal to $g_{t,h}^{DA}$.

In order to demonstrate the process, examples of two wind power PDFs are presented in Figure 1. The wind power is distributed in seven levels with its associated probabilities as shown in Figure 1a, while the wind power is curtailed on its fifth level as shown in Figure 1b, and the probabilities of level 6 and 7 are added to level 5. Please note that a higher total wind curtailment level means less wind power curtailment. Therefore, there is no curtailment if the wind power curtailment level is chosen 7.

Moreover, there are some constraints related to $Pc_{t,s}^{DA}$ as follows:

$$Pc_{t,s}^{DA} = Pc_{t,s}^{DA,Dis} + Pc_{t,s}^{DA,Sim} - Pc_{t,s}^{DA,Cha} \quad \forall t,\ \forall s \tag{6}$$

The power limits of CAES in different operation modes are as follows:

$$0 \le Pc_{t,s}^{DA,Cha} \le P_{Com}^{Max}.Uc_{t,s}^{DA,Cha} \quad \forall t,\ \forall s \tag{7}$$

$$0 \le Pc_{t,s}^{DA,Sim} \le Pc_{Exp}^{Max}.Uc_{t,s}^{DA,Sim} \quad \forall t,\ \forall s \tag{8}$$

$$0 \le Pc_{t,s}^{DA,Dis} \le Pc_{Exp}^{Max}.Uc_{t,s}^{DA,Dis} \quad \forall t,\ \forall s \tag{9}$$

As formulated in Equation (10), the CAES may operate in one of these modes at each period.

$$Uc_{t,s}^{DA,Dis} + Uc_{t,s}^{DA,Sim} + Uc_{t,s}^{DA,Cha} \le 1 \quad \forall t,\ \forall s \tag{10}$$

No uncertainty is assumed for CAES power generation. The CAES energy level (i.e. state-transition equation) is modelled as follows:

$$Ec_{t,s}^{DA} = Ec_{t-1,s}^{DA} + Er\left(Pc_{t,s}^{DA,Cha} - Pc_{t,s}^{DA,Dis}\right) \quad \forall t > 1,\ \forall s \tag{11}$$

$$Ec_{1,s}^{DA} = Ec_{24,s}^{DA} = Ec^{INT} \quad \forall s \tag{12}$$

$$Ec^{Min} \le Ec_{t,s}^{DA} \le Ec^{Max} \quad \forall t,\ \forall s \tag{13}$$

To include the non-decreasing curves for DA market bidding, the following constraints are defined [5]:

$$\left(Ph_{t,s}^{DA} - Ph_{t,s'}^{DA}\right).\left(\rho_{t,s}^{DA} - \rho_{t,s'}^{DA}\right) \ge 0 \quad \forall t,\ \forall s,\ \forall s' \tag{14}$$

$$Ph_{t,s}^{DA} = Ph_{t,s'}^{DA} \quad \forall t,\ \forall s,\ \forall s' \ :\ \rho_{t,s}^{DA} = \rho_{t,s'}^{DA} \tag{15}$$

Finally, the equation related to the operational cost of CAES can be written as follows:

$$\begin{aligned} OC_{t,s} = {} & Pc_{t,s}^{DA,Dis}\left(Hc^{Dis}.NG + Qc^{Exp}\right) \\ & + Pc_{t,s}^{DA,Sim}\left(Hc^{Sim}.NG + Qc^{Exp} + Qc^{Com}\right) \\ & + Pc_{t,s}^{DA,Cha} Qc^{Com} \quad \forall t,\ \forall s \end{aligned} \tag{16}$$

The second objective function considered is voltage stability improvement. The static voltage stability margin can be defined through the minimal $\mathcal{K}$ index [23, 24]:

$$\bar{K}_j = \left| 1 - \sum_{i \epsilon B_G} И_{ji} \frac{V_i}{V_j} \right| \quad j \epsilon B_L \tag{17}$$

where B_L and B_G are the sets of load buses and generator buses, respectively. $\bar{\mathcal{K}}_j$ represents the impact of the voltage magnitude of PV buses (buses connected to the generator) on the voltage magnitude of PQ buses (load buses) in the power system based on the admittance matrix ($И$). $\bar{\mathcal{K}}_j$ is only calculated for load buses in which the risk of voltage collapse is higher than the PV buses. The matrix ($И$) can be calculated as:

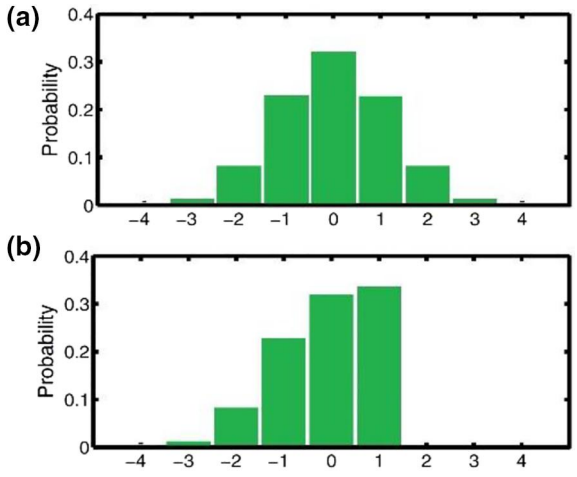

FIGURE 1 (a) Initial wind power PDF; (b) the curtailed wind power PDF

$$[M] = -[Y_{LL}]^{-1}[Y_{LG}] \tag{18}$$

where $[Y_{LL}]$ and $[Y_{LG}]$ are the submatrices of the admittance matrix $Y_{bus} = \begin{bmatrix} Y_{LL} & Y_{LG} \\ Y_{GL} & Y_{GG} \end{bmatrix}$ partitioned in accordance with the B_L and B_G.

In stable conditions, $\bar{K}_j$ indices are required to be between 0 and 1. Therefore, an overall indicator $\bar{K}$ that defines the stability of the whole system can be transcribed as the maximum of the $\bar{K}_j$ indices; it gives the closeness of the system to voltage collapse. The minimum of this overall indicator can be defined as an objective function as shown in Equation (19):

$$\begin{aligned} &\min_{\Theta b_{t,s}} \mathcal{Z}_2 \\ &\mathcal{Z}_2 = \bar{K} = \max(K_j) \quad j \in B_L \end{aligned} \tag{19}$$

It should be noted that although the presented voltage stability improvement index and voltage profile improvement index [25] both improve the voltage in the system, they have major differences. Specifically, the voltage profile index, which is usually defined as $\sum_{j \in Bl} |1 - V_j|$, represents the deviation of the voltage of the load buses from the nominal voltage (1 p.u.). This index is unable to show how far is the voltage magnitude from the stability margin. Therefore, we use the above index in Equation (17) for voltage stability improvement.

The third objective function considered is congestion management. For the sake of simplicity, it is assumed that the maximum power capacity of each line is the same. In order to consider congestion management in the problem, we try to minimize the maximum power through the lines of the network. Also, a penalty factor is implemented to eliminate the solutions which lead to congestion through the network. The powers through the lines of the network can be written as:

$$P_{line} = [P_1 \quad P_2 \quad P_3 \quad \dots \quad P_{N_{line}}], \tag{20}$$

To reject the solutions which lead to congestions, the relevant penalty factor can be formulated using:

$$BP_l = \begin{cases} 0 & P_l \le P_l^{max} \\ 1 & P_l > P_l^{max} \end{cases} \quad , \forall l \epsilon [1,\ 2,\ \dots, N_{line}] \tag{21}$$

$$Penalty\ factor = m \times \sum_{l=1}^{N_{line}} BP_l \tag{22}$$

As mentioned earlier, the maximum power capacity of all lines is presumed to be equal. Therefore, the third objective function, which is to minimize the maximum power through the lines of the network, can be written as in Equation (23). Note that if the maximum amount of power in lines is different, the normalized value of power passing through the line can be considered in the formulation.

$$\begin{aligned} &\min_{\Theta b_{t,s}} \mathcal{Z}_3 \\ &\mathcal{Z}_3 = \max(P_{line}) + Penalty\ factor \end{aligned} \tag{23}$$

Usually, there is only one line that has the maximum power passing through it. If the power in this line is reduced, the overall power through all lines will be reduced.

2.1 | Equality constraints

The optimal power flow equality constraints, including active and reactive powers, can be written as the following equations:

$$P_{gi} - P_{di} = \sum_{j=1}^{n_b} V_i V_j \left(G_{ij} cos\theta_{ij} + B_{ij} sin\theta_{ij}\right) \tag{24}$$

$$Q_{gi} - Q_{di} = \sum_{j=1}^{n_b} V_i V_j \left(G_{ij} sin\theta_{ij} - B_{ij} cos\theta_{ij}\right) \tag{25}$$

where G_{ij} and B_{ij} are the real and imaginary parts of the network admittance matrix element Y_{ij}, respectively, so that $Y_{ij} = G_{ij} + jB_{ij}$. P_{gi} and P_{di} are the real power generation and consumption of the i-th bus. Q_{gi} and Q_{di} are the reactive power generation and consumption of the i-th bus. θ_{ij} is the voltage angle difference between bus i and bus j.

2.2 | Inequality constraints

The optimal power flow inequality constraints include active and reactive power generation of each generator (Equations 26 and 27), and the voltage profile of each load bus (Equation 28).

$$P_{gi\ min} \le P_{gi} \le P_{gi\ max} \quad i \in B_G \tag{26}$$

$$Q_{gi\ min} \le Q_{gi} \le Q_{gi\ max} \quad i \in B_G \tag{27}$$

$$V_{i\ min} \le V_i \le V_{i\ max} \quad i \in B_L \tag{28}$$

Note that Matpower M-file package is used to solve the optimal power flow. Equality and inequality constraints are completely satisfied in the process of solving optimal power flow with Matpower.

2.3 | Multi-objective strategy and optimization tool

In this section, the multi-objective technique and its concept are introduced. Figure 2 shows the concept of multi-objective Pareto solutions for three objective functions. As shown in this figure, all populations are arranged with the best values of the objective functions, and the non-dominated solutions are identified (black dots).

The values of the objective functions are usually quite different. For example, in this study, the profit maximization objective function values are about 1 million, and voltage stability objective function values are between 0 and 1. Hence, solutions are derived in sequence based on the range of the objective functions. In other words, the solutions with the biggest range objective function (congestion management) are calculated first, and the solutions with the smallest range objective function (negative market profit) are lastly calculated. The reason that the negative value of the market profit is considered is that this objective function is required to be maximized, on the contrary, to the other objective functions (congestion management and voltage stability index [VSI]). Note that for calculating the objective function in each iteration, the optimal power flow is performed using Matpower.

After finding the multi-objective Pareto solutions, the operator might want to select the best compromise solution [26]. Thus, the fuzzy method is used to find this solution. In the fuzzy method, first, a normalization method is defined to equalize the range for the three objective functions and put them between 0 and 1. This procedure is formulated as:

$$Norm_{Z_{k,s}} = \begin{cases} 1 & Z_{k,s} \le Z_k^{min} \\ \dfrac{Z_k^{max} - Z_{k,s}}{Z_k^{max} - Z_k^{min}} & Z_k^{min} < Z_{k,s} < Z_k^{max} \\ 0 & Z_{k,s} \ge Z_k^{max} \end{cases} \tag{29}$$

where Z_k^{max} and Z_k^{min} are the value of k-th objective function which is completely unsatisfactory and satisfactory to the decision-maker, respectively. $Z_{k,s}$ and $Norm_{Z_{k,s}}$ are the s-th non-dominated solution of k-th objective function and its normalized value which has the values between 0 and 1, respectively.

The membership function can be determined for each individual as follows:

$$\varpi_s = \frac{\sum_{k=1}^{N_Z} \omega_k \times Norm_{Z_{k,s}}}{\sum_{i=1}^{N_{sol}} \sum_{k=1}^{N_Z} \omega_k \times Norm_{Z_{k,i}}} \tag{30}$$

where ϖ_s is the membership function of s-th non-dominated solution. ω_k is the weighting factor of the k-th objective function. For calculating the best compromise solution, the weighting factor for each objective function is assumed to be the same which is equal to 0.33 to calculate the best compromise solution. This means all the objection functions have the same importance for the decision-maker. The solution with the maximum membership ϖ_s is the best compromise solution [26]. The procedure is also shown as a flowchart in Figure 3. Please note that i_{max} is the maximum number of iterations in the algorithm. An enhanced Jaya algorithm called LJaya-TVAC algorithm, which is based on time-varying acceleration coefficients and learning phase introduced in Teaching-Learning-Based Optimization (TLBO), is used to solve the optimization problem. Jaya is a powerful algorithm based on the conception that the new solution moves in the direction of the previously found best solution and escapes from the worst one. Jaya algorithm only needs the common control parameters and has no algorithm-specific control parameters. However, for higher convergence rate, variable coefficients and the learning phase in TLBO is added to the Jaya algorithm. The detail about the Jaya and LJaya-TVAC algorithm is available in [21, 27].

3 | CASE STUDY

The 57-bus test system is used to test the proposed approach which consists of seven generator units at buses 1, 2, 3, 6, 8, 9, and 12. The data related to the 57-bus test system can be found in [28]. The network in which the HPP including WPA and CAES aggregator is tested is shown in Figure 4. In this figure, the red and blue circles indicate the CAES and wind power plants, respectively. The presented approach determines a coordinated operation for HPP (i.e. including a WPA and a CAES aggregator). The CAES units employ the simple cycle mode to maximize their profit. The wind power and DA

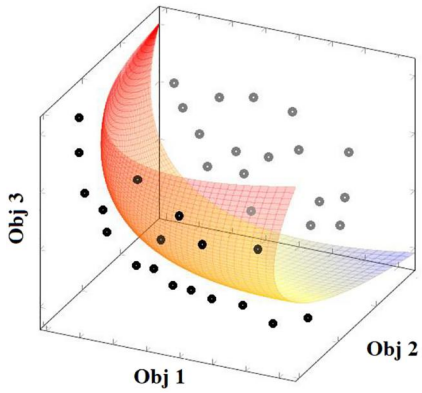

FIGURE 2 Pareto-optimal front concept for three objective functions

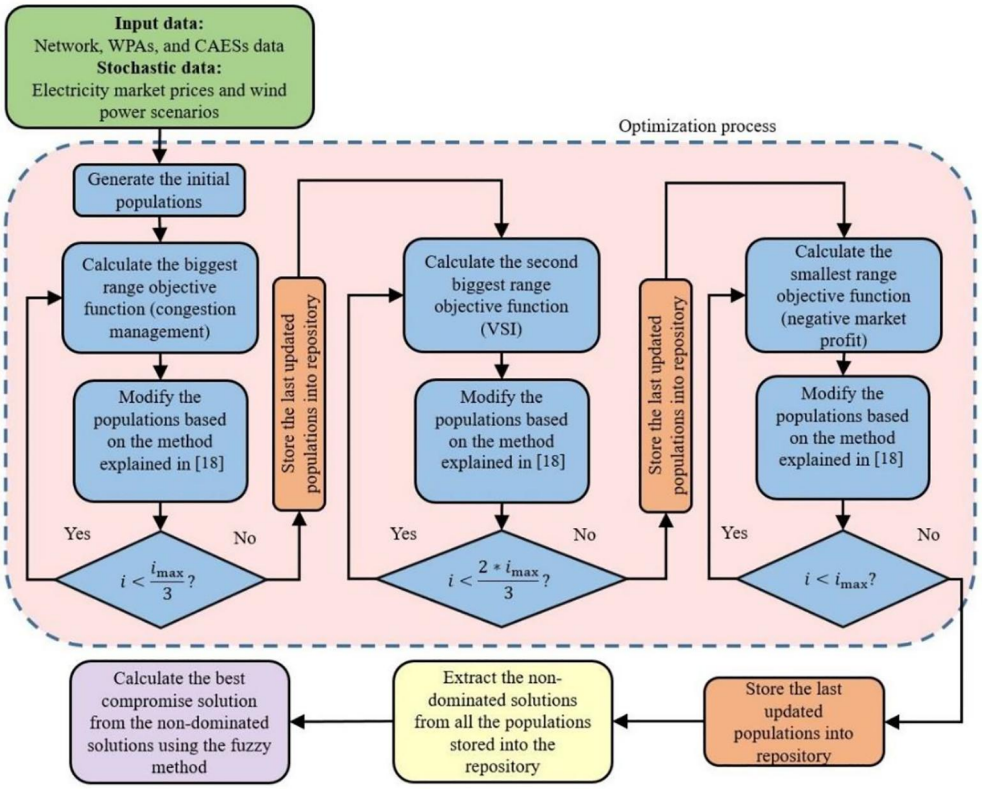

FIGURE 3 The optimization framework

FIGURE 4 Diagram illustration of system configurations

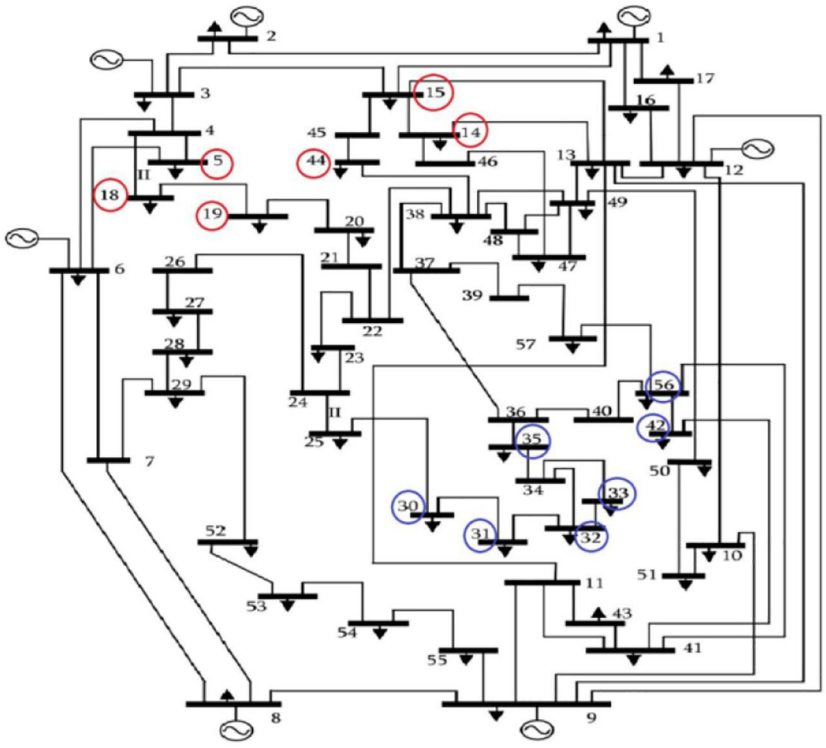

market price uncertainties are modelled using the scenario generation and reduction method which are explained as follows: N_1, and N_2 scenarios are generated for wind power generation, and DA market price, respectively. These uncertainty sources are independent uncertainty parameters. Also, the symmetric scenario tree is implemented to construct

$N_S = N_1 \times N_2$ scenarios based on the wind power (N_1) and DA market price (N_2) scenarios. The presented procedure is applied to the Sotavento wind farm [29] located in Spain. The artificial neural network is trained by the wind power real data records of the year 2010. The scenarios related to market prices are obtained by the following procedure: Firstly, the prediction of DA market price for 30 days is derived by an adapted hybrid neural network and an improved Jaya algorithm [21, 30]. Secondly, the estimation of the error probability distribution function (PDF) is calculated for each hour. Finally, based on these estimations, 1000 scenarios are produced by applying the roulette wheel mechanism for each of the wind and DA market price. Also, the scenario reduction method is employed to diminish the number of scenarios to 30 ($N_1 = 30$ and $N_2 = 30$) by removing similar scenarios in addition to very low probable scenarios using the fast forward algorithm [31]. The error variance of 10% is used in the article for both wind and DA market price scenario generations.

The proposed method is applied on six aggregated wind farms with 7 MW capacity for each. The maximum capacity of 15 MW is considered for each of six CAES units depicted in Figure 4. Values of 0.4185 and 0.837 are considered for CAESs heat rate in discharging and simple cycle modes, respectively [32]. The price of natural gas is considered to be 3.5 €/GJ. Besides, the equal value of 0.87 €/kWh is considered for variable operation and maintenance cost in both modes of expansion and compression, respectively. The air storage capacity of CAES cavern can reach to 15 and one MWh at the highest and lowest level, respectively. The energy level of 1 MWh is considered for the initial stored energy of CAES cavern, while CAES energy conversion ratio is 0.95 for both compression and expansion modes. P_l^{max} is considered to be equal to 200 MW. Figure 5 also shows the electricity price profile.

Figure 6a demonstrates the non-dominated and best compromise solutions for the pitch angle control and charging and discharging levels of CAESs and WPs that are optimally achieved by an improved Jaya algorithm for three objective functions including congestion management, voltage stability enhancement, and market profit maximization. Also, as shown in the figure, the best compromise solution is designated by a bigger blue star. This solution is obtained

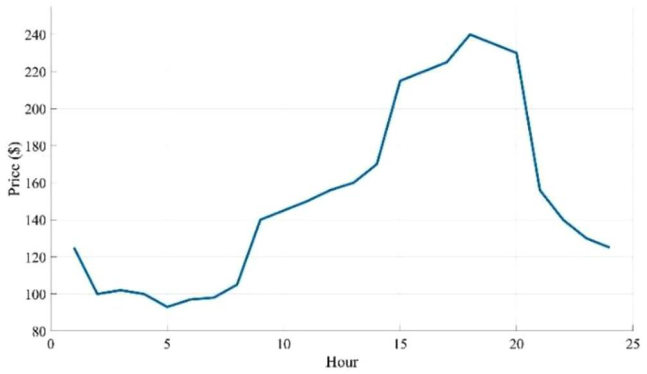

FIGURE 5 Electricity price profile

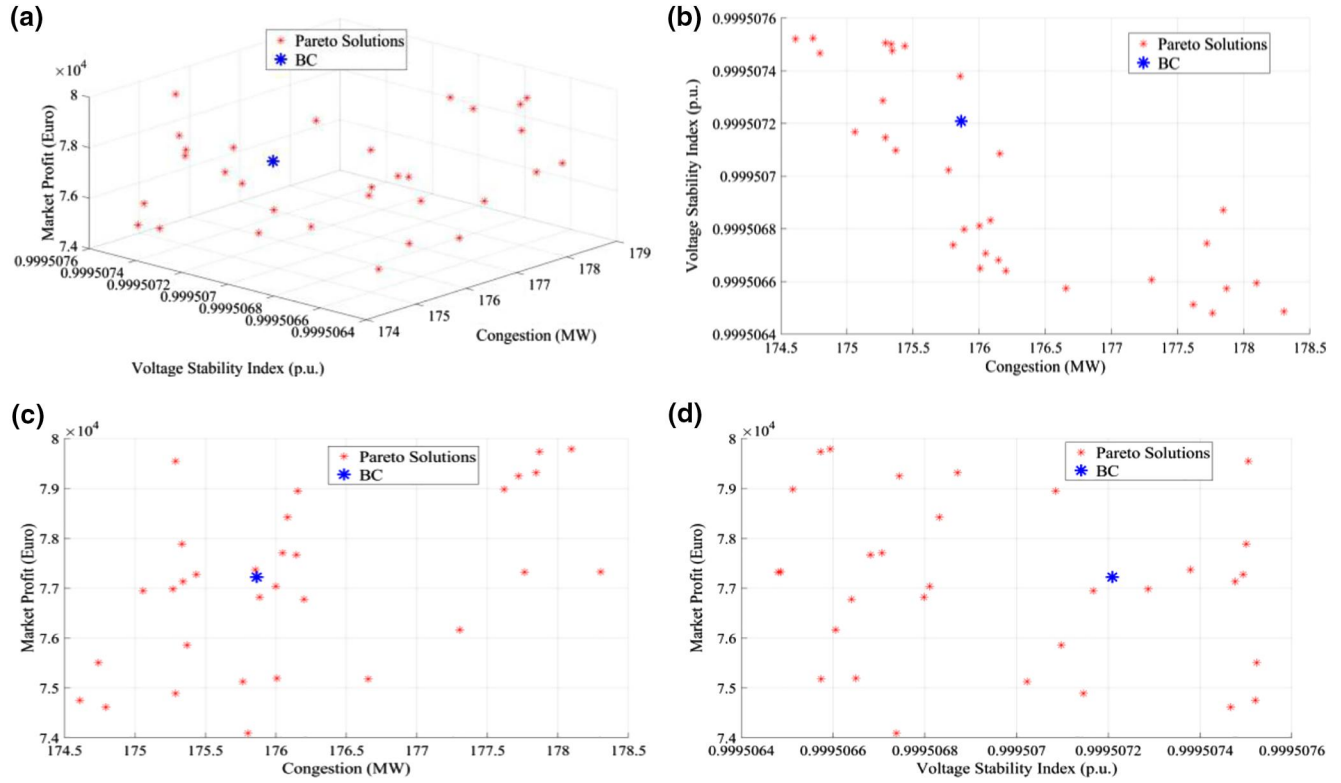

FIGURE 6 Three-dimensional view Pareto front for market profit, VSI, and congestion (a). Two-dimensional view Pareto front for VSI and congestion (b), market profit and congestion (c), and market profit and VSI (d)

using the fuzzy method, which is explained in more detail in Section 2.3. In the solution that is best for congestion management, the amount of market profit, which includes WPA and CAES aggregator, VSI, and congestion are 74,750, 0.99950752, and 174.6096, respectively. This means that the maximum power passing through the worst congested line is reduced to 174.6096 MW.

In the solution that has the maximum market profit, the amount of market profit, VSI, and congestion are 79,787, 0.99950659, and 178.0979, respectively. Also, in the solution that the voltage stability has the minimum value, which is the best one, the amount of market profit, VSI, and congestion are 77,322, 0.99950648, and 177.7645, respectively. For the best compromise solution, the amount of market profit, VSI, and congestion are 77,223, 0.99950720, and 175.8644 (this means that for the worse congested line, the maximum power passing through that line is reduced to 175.8644 MW), respectively. Congestion management index, VSI, and market profit value for different weighting factors for each objective function are tabulated in Table 1. Note that ω_1, ω_2, ω_3 in the table refer to weighting factors of market profit, VSI, and congestion management index, respectively.

In order to clearly see the values of objective functions, Figure 6a is also shown in two dimensions in Figure 6b–d.

TABLE 1 Congestion management index, VSI, and market profit value for the best solutions for each and the best compromise solution

ω_1	ω_2	ω_3	Market Profit ($)	VSI	Congestion Management (MW)
0.33	0.33	0.33	77,223	0.99950720	175.8644
0	0	1	74,750	0.99950752	174.6096
0	1	0	77,322	0.99950648	177.7645
1	0	0	79,787	0.99950659	178.0979
0	0.5	0.5	75,191	0.99950665	176.0082
0.5	0	0.5	76,949	0.99950717	175.0590
0.5	0.5	0	78,983	0.99950650	177.6191

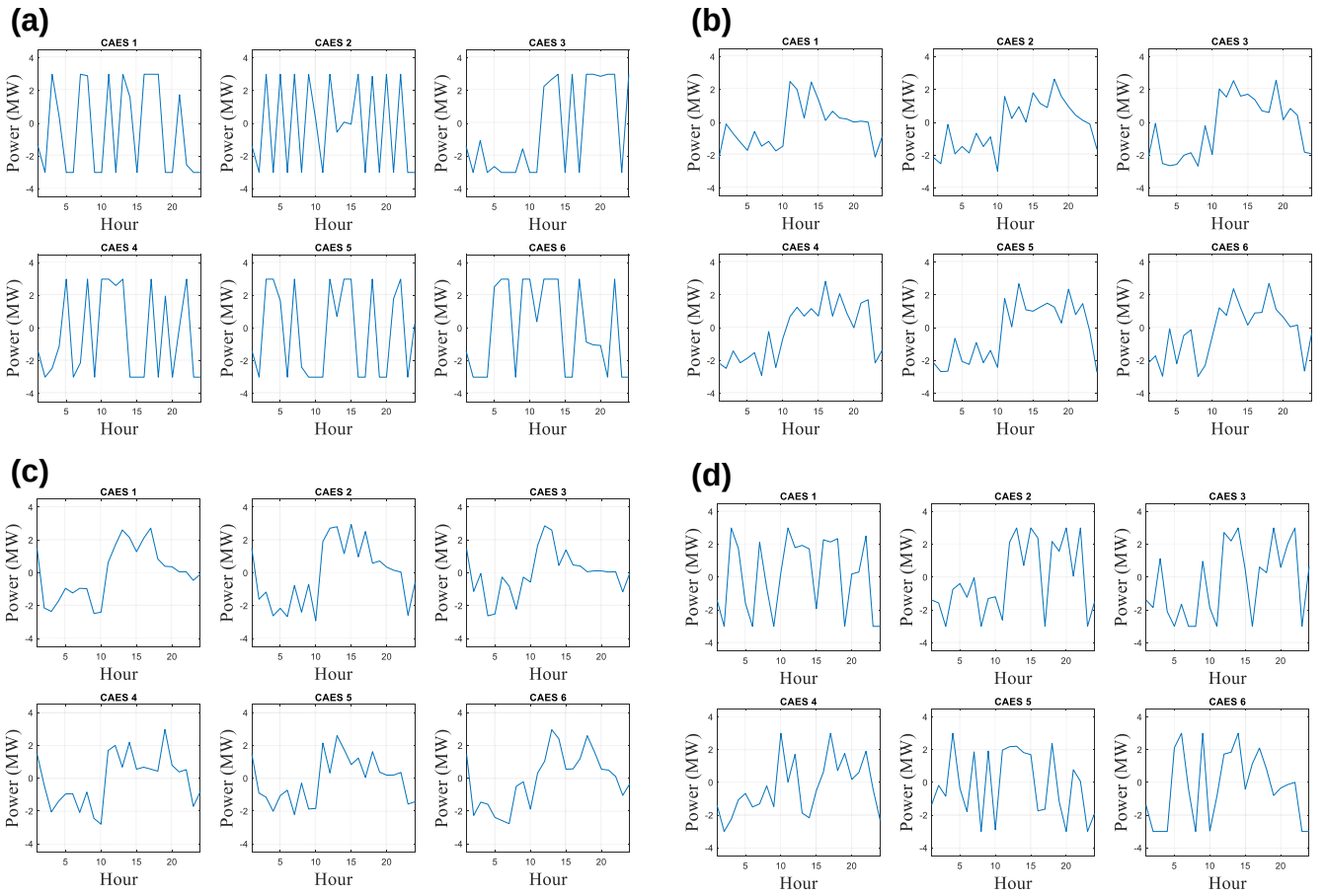

FIGURE 7 CAESs charging and discharging for (a) minimum congestion (b) minimum VSI (c) maximum profit (d) best compromise solution

The obtained optimal schemes of CAES caverns' charging/discharging for all installed CAESs are shown in Figure 7a–d. The objective function to be optimized for Figure 7a is the minimum congestion. The negative values of this figure signify the charging of the cavern, whereas the positive values indicate the discharging. Figure 7b shows the optimal CAES caverns' charging and discharging of the six installed CAESs for the minimum VSI as the objective function. In order to have a better stability boundary, the demand load needs to be locally served [33].

The maximization of electricity market profit is the objective function for Figure 7c. The variation of charging and discharging of the cavern is mostly associated with the variation of the hourly electricity prices. Figure 7d shows the optimal CAES caverns' charging and discharging for the best compromise solution. As mentioned earlier, all the objective functions are equally optimized using fuzzy method to achieve the best compromise solution.

Figure 8 also shows the optimal power bids of the HPP in the DA market for different objective functions and the best compromise solution. As seen from the figure, for the best

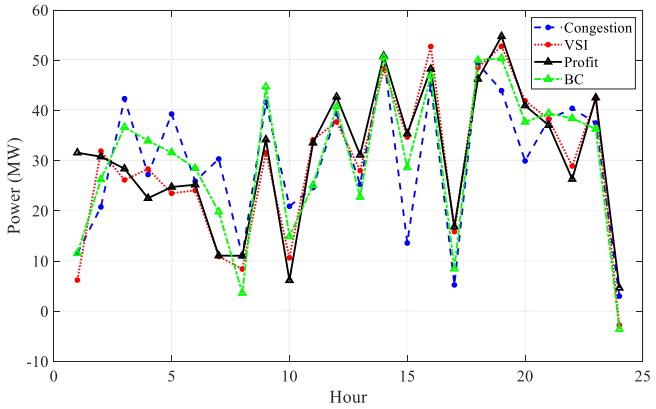

FIGURE 8 Optimal power bids of the HPP in the DA market for different objective functions

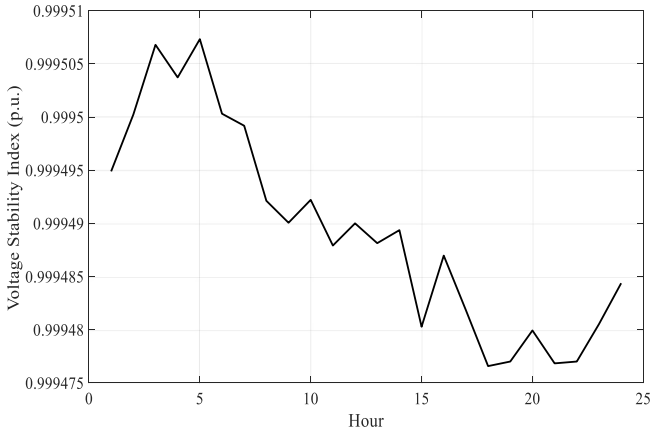

FIGURE 9 VSI during the 24-h time horizon

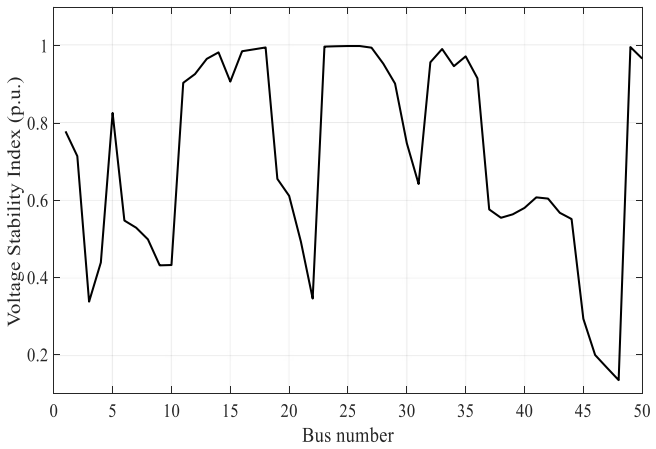

FIGURE 10 The bus-VSI profile at hour #5

TABLE 2 Wind curtailment level for (a) congestion management objective function (b) VSI objective function (c) profit maximization objective function (d) the best compromise solution

(a)

Hour	WP 1	WP 2	WP 3	WP 4	WP 5	WP 6	WP 7
1	7	1	1	1	1	7	7
2	1	1	1	1	7	7	1
3	1	7	1	7	1	7	1
4	7	1	7	1	7	7	7
5	7	6	1	1	1	1	7
6	7	7	7	7	1	7	7
7	1	7	7	1	3	1	1
8	7	1	7	1	1	3	7
9	1	7	1	1	7	1	1
10	1	7	7	1	1	5	1
11	7	7	1	7	7	7	7
12	1	1	7	7	7	7	1
13	7	2	7	2	1	6	7
14	1	1	7	1	7	7	1
15	7	1	7	1	7	4	7
16	1	7	7	1	1	1	1
17	6	1	7	7	1	1	6
18	1	7	2	1	1	7	1
19	1	1	7	1	1	4	1
20	7	7	7	1	7	7	7
21	1	7	1	7	7	7	1
22	1	7	7	1	7	7	1
23	1	1	7	7	1	1	1
24	1	1	1	2	7	7	1

(b)

Hour	WP 1	WP 2	WP 3	WP 4	WP 5	WP 6	WP 7
1	2	4	5	4	2	5	2
2	1	2	6	3	7	3	1
3	4	3	7	4	6	2	4
4	6	5	6	7	6	6	6
5	3	5	3	7	3	7	3
6	2	1	6	7	2	2	2
7	5	7	4	1	2	6	5
8	1	5	2	6	7	2	1
9	5	1	5	1	4	7	5
10	1	3	1	1	1	2	1
11	3	7	2	2	2	5	3
12	3	7	1	4	3	5	3
13	6	2	4	7	2	7	6
14	2	1	2	3	2	6	2
15	5	7	3	6	6	4	5
16	5	3	4	4	6	1	5
17	2	5	6	2	5	3	2
18	3	3	5	5	5	2	3
19	7	6	3	4	6	5	7
20	5	6	7	7	2	3	5
21	7	5	2	4	1	6	7
22	3	2	7	4	3	7	3
23	5	4	3	2	1	6	5
24	2	6	3	5	7	7	2

(c)

Hour	WP 1	WP 2	WP 3	WP 4	WP 5	WP 6	WP 7
1	7	2	3	2	1	6	7
2	5	2	6	4	4	3	5
3	2	4	6	4	4	2	2
4	6	2	5	1	3	1	6
5	5	3	3	6	3	4	5
6	6	4	7	4	5	5	6
7	5	2	4	2	6	5	5
8	7	6	4	2	7	7	7
9	3	2	3	7	3	1	3
10	3	4	5	1	6	4	3
11	2	3	7	7	5	4	2
12	5	6	3	3	3	5	5

(Continues)

TABLE 2 (Continued)

(c)

Hour	WP 1	WP 2	WP 3	WP 4	WP 5	WP 6	WP 7
13	2	5	4	6	7	6	2
14	4	3	2	6	2	4	4
15	4	5	5	1	7	2	4
16	6	6	7	4	7	7	6
17	6	6	6	2	4	1	6
18	2	7	2	1	3	1	2
19	5	1	3	3	7	3	5
20	1	2	3	7	5	1	1
21	3	3	6	6	1	5	3
22	1	7	5	3	6	7	1
23	5	5	5	1	5	3	5
24	3	6	2	4	6	5	3

(d)

Hour	WP 1	WP 2	WP 3	WP 4	WP 5	WP 6	WP 7
1	7	4	4	1	1	1	7
2	6	2	1	1	7	7	6
3	2	7	7	6	1	7	2
4	1	2	5	4	7	5	1
5	5	5	1	3	1	5	5
6	7	7	6	5	1	6	7
7	1	7	7	3	7	1	1
8	6	1	7	6	7	7	6
9	4	1	1	1	6	2	4
10	1	5	6	1	1	4	1
11	4	4	1	7	2	7	4
12	7	7	7	7	3	2	7
13	5	5	1	7	3	1	5
14	1	1	7	3	7	3	1
15	3	6	5	1	1	2	3
16	1	7	7	5	6	7	1
17	6	3	2	1	4	5	6
18	5	5	7	1	1	4	5
19	1	6	5	1	3	1	1
20	5	7	7	1	7	7	5
21	1	6	3	5	4	5	1
22	2	7	7	1	7	4	2
23	1	6	7	7	5	2	1
24	2	7	3	1	5	7	2

solution for market profit, the HPP prefers to sell the electricity in peak hours which are more expensive.

Figure 9 shows the 24-h profile of the grid voltage stability. As can be seen, hour #5 has the worst voltage stability. Furthermore, the bus-VSI profile at hour #5 and the worst bus-VSI are shown in Figure 10. The bus 26 has the worst bus-VSI (bus 31 considered as the generator bus) with the value of 0.99950734 p.u.

The hourly wind curtailment levels for four solutions including the best solution for congestion management, the best solution for VSI, the best solution for electricity market profit and the best compromise solution are shown in Table 2a–d. The total wind curtailment level of the best solution for congestion management is the smallest among the other mentioned solutions with a value of 573. The total wind curtailment level of the best solution for profit maximization is 589. The total wind curtailment level of the best solution for VSI is 585. Also, the total wind curtailment level of the best compromise solution is the largest among the other mentioned solutions with a value of 594. Please note that the maximum number of wind curtailment level is 7, and when the curtailment level is 7, it means there is no curtailment.

It can be seen from the results that even though the wind power is totally free, there are intervals in which WPAs are not permitted to inject the entire obtainable wind powers to the network and sell to the electricity markets. The reason is that for satisfying objective functions other than market profit maximization such as congestion management, the wind power generation needs to be curtailed for some hours in which some wind generators produce more than enough such that some lines are congested.

4 | CONCLUSION

This article has modelled an HPP considering network WPA. The wind generators are equipped with pitch angle control ability to adjust the wind power curtailment level. In order to analyse the effects of the network constraints, two additional objective functions including congestion management and voltage stability improvement have been considered, and multi-objective Pareto front solutions have been used to optimize all the objective functions simultaneously. The results show that these two additional technical objectives conflict with the profit maximization in the electricity market. This method is used in the time that the market player gets benefits or incentives from the network owner by bringing congestion management and voltage stability indices to a specific point.

Two different technical objectives from the perspective of the power grid were considered. The problem can also be solved in the future study based on other objectives such as power losses and voltage profile of the network.

NOMENCLATURE

Definitions

CVaR	Conditional Value-at-Risk
WPA	Wind Power Aggregator
CAES	Compressed Air Energy Storage
HPP	Hybrid Power Plant

Indices

1) Sets

s	Index of scenario
T	Index of time
H	Index of wind power discrete level

Superscripts

Cha	Index for charging mode of CAES
DA	Index for offered power to day-ahead market
Dis	Index for discharging mode of CAES
INT	Index for initial value
Sim	Index for simple-cycle mode of CAES

Constants

B_L	Set of load buses
B_G	Set of generator buses
N_s	Total number of scenarios
N_T	Total period of time
N_{line}	Total number of lines in the network
N_{sol}	Total number of non-dominated solutions
N_Z	Total number of objective functions
π_s	Probability of occurrence of scenario s
ζ	Risk-aversion factor
σ	Confidence level with $\sigma \in (0,1)$
P_l	Power passing from end to end of the line l
P_l^{max}	Maximum power capacity that can be passed from end to end of the line l
Pw^{Max}	Maximum capacity of WPA
$Pc_{Exp/Com}^{Max}$	Maximum expanding/compressing capacity of CAES
m	A sufficiently large number (e.g. 10^{100})
Er	CAES energy ratio for converting power to energy in cavern
$Ec^{Max/Min}$	Maximum/minimum schedulable level of energy in CAES cavern
Hc	CAES heat rate in one of operating modes
NG	Natural gas price

Variables

Ph	Power produced by HPP
Pw	Power produced by WPA
Pc	Power produced by CAES
ρ	Price of electricity
$\beth$	Wind curtailment decision variable
g	Discrete realization of wind power
$OC_{t,s}$	Total operational cost of CAES
Uc	Binary variable to show ON/OFF operating status of CAES
Ec	Scheduled energy level of the CAES
$Qc^{Exp/Com}$	CAES variable operation and maintenance cost for expanding/compressing modes

REFERENCES

1. Fertig, E., Apt, J.: Economics of compressed air energy storage to integrate wind power: a case study in ERCOT. Energy Pol. 39(5), 2330–2342 (2011)
2. Shafiee, S., et al.: Risk-constrained bidding and offering strategy for a merchant compressed air energy storage plant. IEEE Trans. Power Syst. (2016)
3. Shafiee, S., et al.: Risk-constrained bidding and offering strategy for a merchant compressed air energy storage plant. IEEE Trans. Power Syst. 32(2), 946–957(2017)
4. Black, M., Strbac, G.: Value of bulk energy storage for managing wind power fluctuations. IEEE Trans. Energy Convers. 22(1), 197–205 (2007)
5. Morales, J.M., Conejo, A.J., Pérez-Ruiz, J.: Short-term trading for a wind power producer. IEEE Trans. Power Syst. 25(1), 554–564 (2010)
6. Baringo, L., Conejo, A.J.: Strategic offering for a wind power producer. IEEE Trans. Power Syst. 28(4), 4645–4654 (2013)
7. Zugno, M., et al.: Pool strategy of a price-maker wind power producer. IEEE Trans. Power Syst. 28(3), 3440–3450 (2013)
8. Nikoobakht, A., et al.: Flexible co-scheduling of integrated electrical and gas energy networks under continuous and discrete uncertainties. Energy, 182, 201–210 (2019)
9. Nikoobakht, A., et al.: Decentralised hybrid robust/stochastic expansion planning in coordinated transmission and active distribution networks for hosting large-scale wind energy. IET Gener. Transm. Distrib. (2019)
10. Güçyetmez, M., Çam, E.: A new hybrid algorithm with genetic-teaching learning optimization (G-TLBO) technique for optimising of power flow in wind-thermal power systems. Electr. Eng. 98(2), 145–157 (2016)
11. Garcia-Gonzalez, J., et al.: Stochastic joint optimization of wind generation and pumped-storage units in an electricity market. IEEE Trans. Power Syst. 23(2), 460–468 (2008)
12. de la Nieta, A.A.S., Contreras, J., Munoz, J.I.: Optimal coordinated wind-hydro bidding strategies in day-ahead markets. IEEE Trans. Power Syst. 28(2), 798–809 (2019)
13. Greenblatt, J.B., et al.: Baseload wind energy: modelling the competition between gas turbines and compressed air energy storage for supplemental generation. Energy Pol. 35(3), 1474–1492 (2007)
14. Mohammadi, J., Rahimi-Kian, A., Ghazizadeh, M.-S.: Aggregated wind power and flexible load offering strategy," IET Renew. Power Gener. 5(6), 439–447 (2011)
15. Zhang, X.: Optimal scheduling of critical peak pricing considering wind commitment. IEEE Trans. Sustain. Energy, 5(2), 637–645 (2014)
16. Heydarian-Forushani, E., et al.: Risk-constrained offering strategy of wind power producers considering intraday demand response exchange. IEEE Trans. Sustain. Energy, 5(4), 1036–1047 (2014)
17. Rabiee, A., et al.: Corrective voltage control scheme considering demand response and stochastic wind power. IEEE Trans. Power Syst. 29(6), 2965–2973 (2014)
18. Hemmati, R., Wu, F., El-Refaie, A.: Survey of insulation systems in electrical machines. In: 2019 IEEE International Electric Machines & Drives Conference (IEMDC), pp. 2069-2076. IEEE (2019)
19. Morshed, M.J., Hmida, J.B., Fekih, A.: A probabilistic multi-objective approach for power flow optimization in hybrid wind-PV-PEV systems. Appl. Energy, 211, 1136–1149 (2018)
20. Teeparthi, K., Kumar, D.V.: Security-constrained optimal power flow with wind and thermal power generators using fuzzy adaptive artificial physics optimization algorithm. Neural Comput. Appl. 29(3), 855–871 (2018)
21. Ghavidel, S., Azizivahed, A., Li, L.: A hybrid Jaya algorithm for reliability–redundancy allocation problems. Eng. Optim. 50(4), 698–715 (2018)
22. Azizipanah-Abarghooee, R., et al.: Corrective economic dispatch and operational cycles for probabilistic unit commitment with demand response and high wind power. Appl. Energy. 182, 634–651 (2016)
23. Kumari, M.S., Maheswarapu, S.: Enhanced genetic algorithm based computation technique for multi-objective optimal power flow solution. Int. J. Electr. Power Energy Syst. 32(6), 736–742 (2010)
24. Niknam, T., et al.: Improved particle swarm optimisation for multi-objective optimal power flow considering the cost, loss, emission and voltage stability index. IET Gener. Transm. Distrib. 6(6), 515–527 (2012)
25. Ghavidel, S., et al.: Static var compensator allocation considering transient stability, voltage profile and losses. In: 2017 20th International Conference on Electrical Machines and Systems (ICEMS), pp. 1–6. IEEE (2017)
26. Wang, L., Singh, C.: Environmental/economic power dispatch using a fuzzified multi-objective particle swarm optimization algorithm. Electr. Power Syst. Res. 77(12), 1654–1664 (2007)
27. Rao, R.: Jaya: a simple and new optimization algorithm for solving constrained and unconstrained optimization problems. Int. J. Ind. Eng. Comput. 7(1), 19–34 (2016)
28. Power systems test case archive. http://www.ee.washington.edu/research/pstca
29. Sotavento wind farm. http://www.sotaventogalicia.com/
30. Aghaei, J., et al.: Risk-constrained offering strategy for aggregated hybrid power plant including wind power producer and demand response provider. IEEE Trans. Sustain. Energy. 7(2), 513–525 (2016)
31. Amjady, N., Aghaei, J., Shayanfar, H. A.: Stochastic multiobjective market clearing of joint energy and reserves auctions ensuring power system security. IEEE Trans. Power Syst. 24(4), 1841–1854 (2009)
32. Shafiee, S., et al.: Risk-constrained bidding and offering strategy for a merchant compressed air energy storage plant. IEEE Trans. Power Syst. 32(2), 946–957 (2016)
33. Azizivahed, A., et al.: Energy storage management strategy in distribution networks utilised by photovoltaic resources. IET Gener. Transm. Distrib. 12(21), 5627–5638 (2018)

How to cite this article: Ghavidel S, Rajabi A, Jabbari Ghadi M, Azizivahed A, Li L, Zhang J. Hybrid power plant bidding strategy for voltage stability improvement, electricity market profit maximization, and congestion management. *IET Energy Syst. Integr.* 2021;3:130–141. https://doi.org/10.1049/esi2.12008